SCIENCE CHINA
Information Sciences

• RESEARCH PAPER •

September 2016, Vol. 59 092205:1–092205:15
doi: 10.1007/s11432-015-5496-2

Sampled-data feedback and stability for a class of uncertain nonlinear systems based on characteristic modeling method

Tiantian JIANG* & Hongxin WU

Science and Technology on Space Intelligent Control Laboratory, Beijing Institute of Control Engineering, Beijing 100190, *China*

Received July 12, 2015; accepted October 28, 2015; published online August 23, 2016

Abstract In this paper, we investigate the tracking problem for a class of second-order uncertain nonlinear systems using sampled-data output feedback. Our controller is designed based on the characteristic modeling method. We first derive the corresponding characteristic model and then give the sampled-data feedback control law, which is referred to as "golden-section adaptive control based on characteristic models". The closed-loop system is shown to be stable and, concurrently, it is demonstrated that the tracking error can be made arbitrarily small by taking a sufficiently small sampling period. Our results improve upon the findings of previous work by removing the persistent excitation condition, and also lay certain theoretical foundations for practical applications of golden-section adaptive control.

Keywords uncertainty, nonlinear system, characteristic model, golden-section adaptive control, sampled-data feedback

Citation Jiang T T, Wu H X. Sampled-data feedback and stability for a class of uncertain nonlinear systems based on characteristic modeling method. Sci China Inf Sci, 2016, 59(9): 092205, doi: 10.1007/s11432-015-5496-2

1 Introduction

Characteristic modeling is a control-oriented modeling method, which considers both the dynamic characteristics of controlled plants and performance specifications [1]. Different to traditional modeling methods, the sole objective of which is to determine plant dynamics as precisely as possible, characteristic modeling aims to establish a simplified model for engineering purposes. However, the characteristics of the controlled plant are not neglected. In general, the resultant characteristic model is described by a low-order slowly time-varying difference equation [1].

As a primary component of characteristic modeling theory, all-coefficient adaptive control based on characteristic models was first proposed by Wu et al. [2, 3], and has since gradually been refined through a number of engineering projects. This technique removes many of the deficiencies of traditional adaptive control theory when applied to practical engineering, while it includes features such as simplicity of design, convenience of adjustment, and strong robustness. To date, the characteristic modeling method has been successfully applied to various engineering projects in the fields of astronautics and industry, e.g., for

* Corresponding author (email: jiangtt@amss.ac.cn)

adaptive re-entry lifting control of manned spacecraft [4], adaptive control of spacecraft instantaneous thermal currents [5], control of an aluminum electrolysis process [6], the automatic rendezvous and docking of the Shenzhou-8 and Shenzhou-9 spacecraft with the Tiangong-1 orbiter [7,8], and for attitude control of spacecraft with deployable and retractable flexible structures [1]. Note that the precision of the re-entry lifting control for manned spacecraft obtained using this technique is of the highest international standard [4].

Important progress has also been made with regard to theoretical research on the characteristic modeling method. In particular, the characteristic modeling problem has been well solved. For high-order linear time-invariant systems and second-order affine nonlinear systems, different characteristic modeling methods have been developed, as reported in [9, 10]. In addition, the equivalence in the output of the resultant characteristic models and controlled plants has been investigated. As regards the closed-loop stability problem, current research is primarily restricted to stability analysis of discrete-time closed-loop systems consisting of characteristic models and corresponding discrete-time controllers (e.g., [1, 11–14]). However, very little research has been conducted on hybrid closed-loop systems comprised of continuous plants and sampled-data controllers. In [15], an adaptive control law was proposed and the stability was proven for a class of affine nonlinear systems with a relative degree of two. However, the stability was verified under a condition of persistent excitation, and it is very difficult to verify such a condition in practice. Recently, sufficient conditions for stability, which are related to the characteristic model-based pole placement method, have been established in [16], including a stringent criterion imposed on characteristic-model modeling errors. Therefore, investigation of the closed-loop stability problem with consideration of appropriate stability conditions is of great significance, both theoretically and practically.

In fact, certain difficulties must be overcome in order to solve the above closed-loop stability problem. Firstly, the resultant characteristic model is typically a time-varying discrete-time system, and the time-varying property causes difficulties with regard to both parameter estimation and stability analysis. Secondly, noting that the characteristic model-based adaptive control is essentially a sampled-data controller, the corresponding closed-loop system can be classed as a hybrid control system. Therefore, in order to prove the system stability, we are required to determine how the proposed sampled-data control can manage the effects of the system's complex structures, uncertainties, and external disturbances on the system performance in a successive sampling period.

In this paper, we discuss the above stability problem, considering the tracking problem for a class of second-order uncertain nonlinear systems. By deriving the characteristic model of a plant, we propose a corresponding golden-section adaptive controller. Then, we demonstrate that this controller can ensure hybrid closed-loop system stability and also make the tracking error sufficiently small, with no persistent excitation requirement. This research lays certain theoretical foundations for practical applications of the characteristic modeling method.

Notation. $\mathbb{R}$ denotes the set of real numbers, $\mathbb{N}$ the set of natural numbers, $\|\cdot\|$ the Euclidean vector norm or the spectral matrix norm [17], and I_m the m-dimensional identity matrix. Let $T > 0$ be the sampling period, $\bullet(k) \triangleq \bullet(t)|_{t=kT}$, $k \in \mathbb{N}$. For any given function $\kappa(t)$, $t \in D_\kappa$, the expression $\kappa(t) = O(1)$, $t \in D_\kappa$ means that there exists a positive constant $M_\kappa > 0$ such that $|\kappa(t)| \leqslant M_\kappa$, $\forall t \in D_\kappa$.

2 Problem formulation

Consider the following single-input-single-output (SISO) second-order nonlinear system:

$$\begin{cases} \dot{x}(t) = Ax(t) + B\left[f(x(t)) + b(t)u(t) + d(t)\right], \\ y(t) = Cx(t), \end{cases} \quad t \geqslant 0, \tag{1}$$

where $x(t) = [x_1(t)\ x_2(t)]^{\mathrm{T}} \in \mathbb{R}^2$, $u(t) \in \mathbb{R}$, and $y(t) \in \mathbb{R}$ are the state variables, the control input, and the measured output, respectively, $f(x)$ is a nonlinear function that may contain unknown dynamics, $b(t)$ is an unknown time-varying parameter, and $d(t)$ represents external disturbances. In addition, the triple

(A, B, C) is defined as

$$A = \begin{bmatrix} 0 & 1 \\ 0 & 0 \end{bmatrix}, \quad B = \begin{bmatrix} 0 \\ 1 \end{bmatrix}, \quad C = [\, 1 \ \ 0 \,].$$

For the uncertain nonlinear system (1), we make the following assumptions.

Assumption 1. The unknown function $f(x)$ is differentiable and globally Lipschitz in x. Moreover, there exists $L > 0$ such that for any $(x_1, x_2)^{\mathrm{T}}$, $(x_1', x_2')^{\mathrm{T}} \in \mathbb{R}^2$,

$$|f(x_1, x_2) - f(x_1', x_2')| \leqslant L\left(|x_1 - x_1'| + |x_2 - x_2'|\right). \tag{2}$$

Assumption 2. The unknown time-varying parameter $b(t)$ is differentiable, belongs to a bounded interval that does not contain 0, and its sign is known. In addition, $\dot{b}(t)$ is bounded. Without loss of generality, let $\underline{b}$, $\bar{b}_1$, and $\bar{b}_2$ be positive constants satisfying

$$0 < \underline{b} \leqslant b(t) \leqslant \bar{b}_1, \ \forall t \in [0, +\infty), \quad \sup_{t \geqslant 0} |\dot{b}(t)| \leqslant \bar{b}_2. \tag{3}$$

Assumption 3. The disturbance $d(t)$ is bounded, i.e., $\sup_{t \geqslant 0} |d(t)| \leqslant d$ with a constant $d > 0$.

For system (1), we consider the output tracking problem. Specifically, our control objective is to develop a sampled-data output feedback controller to ensure that, for all initial states in any given compact set, the output signal $y(t)$ tracks the reference trajectory generated from the target system

$$\dot{x}^*(t) = A_m x^*(t) + Br(t), \quad y^*(t) = Cx^*(t), \quad t \geqslant 0, \tag{4}$$

where the state $x^*(t) \triangleq [x_1^*(t) \ x_2^*(t)]^{\mathrm{T}} \in \mathbb{R}^2$ and the input signal $r(t) \in \mathbb{R}$ satisfies $|r(t)| \leqslant \bar{r}$ with $\bar{r} > 0$ being a known constant. Further, A_m is a Hurwitz matrix defined by

$$A_m = \begin{bmatrix} 0 & 1 \\ -k_1 & -k_2 \end{bmatrix}. \tag{5}$$

Thus, it is apparent from the above that $x^*(t)$ is uniformly bounded, i.e., there exists $M^* > 0$ depending on the system parameters $\{A_m, \bar{r}\}$ and the initial value $x^*(0)$ such that

$$\sup_{t \geqslant 0} \|x^*(t)\| \leqslant M^*. \tag{6}$$

In fact, the above output tracking problem can be equivalently converted into a stabilizing problem for the corresponding error dynamic system, which can simplify the controller design and performance analysis. By introducing the error variables $e_i = x_i - x_i^*$ $(i = 1, 2)$ and $y_e = y - y^*$, and considering the plant given in (1) and the target system given in (4), we can express the error dynamics as

$$\dot{e}_1(t) = e_2(t), \quad \dot{e}_2(t) = F(e_1(t), e_2(t), t) + b(t)u(t), \quad y_e(t) = e_1(t), \tag{7}$$

where $F(e_1, e_2, t) \triangleq f(e_1 + x_1^*(t), e_2 + x_2^*(t)) + d(t) + k_1 x_1^*(t) + k_2 x_2^*(t) - r(t)$, in which $f(\cdot)$ and $d(t)$ are given in (1), and $r(t)$, k_1, and k_2 are given in (4) and (5). Moreover, by Assumptions 1 and 3 and the uniform boundedness of the (x_1^*, x_2^*) state, the following properties of the function $F(\cdot)$ can be easily verified:

(A1) $F(e_1, e_2, t)$ is globally Lipschitz in (e_1, e_2) uniformly in t. Furthermore,

$$\begin{aligned} |F(e_1', e_2', t) - F(e_1'', e_2'', t)| &= |f(e_1' + x_1^*(t), e_2' + x_2^*(t)) - f(e_1'' + x_1^*(t), e_2'' + x_2^*(t))| \\ &\leqslant L(|e_1' - e_1''| + |e_2' - e_2''|), \quad \forall (e_1', e_2')^{\mathrm{T}}, \ (e_1'', e_2'')^{\mathrm{T}} \in \mathbb{R}^2, \ \forall t \geqslant 0. \end{aligned}$$

(A2) $F(0, 0, t)$ is uniformly bounded, i.e., there exists a constant $M_{F0} > 0$ depending on the parameters $\{L, d, k_1, k_2, \bar{r}, M^*\}$ such that

$$\sup_{t \geqslant 0} |F(0, 0, t)| \leqslant M_{F0}. \tag{8}$$

(A3) $F(e_1, e_2, t)$ is differentiable with respect to its arguments, (e_1, e_2). Also,

$$|F(e_1, e_2, t_1) - F(e_1, e_2, t_2)| \leqslant M_{F1}, \ \forall (e_1, e_2)^{\mathrm{T}} \in \mathbb{R}^2, \ \forall t_1, t_2 \geqslant 0, \tag{9}$$

where M_{F1} is a positive number depending on $\{L, d, k_1, k_2, \bar{r}, M^*\}$.

Thus, the tracking problem can be solved by causing the tracking error $y_e(t)$ in (7) to converge to zero. Hence, our control objective becomes the design of a sampled-data output feedback control law to ensure that $y_e(t) \to 0$ as $t \to \infty$.

3 Primary results

In this section, we first present the sampled-data feedback controller and then show our primary results.

3.1 Golden-section adaptive control based on characteristic models

The explicit controller design method, which is referred to as "golden-section adaptive control based on characteristic models" was initially developed by Wu and presented in [2]. Before proceeding further, considering that our control objective is now to ensure that $y_e(t)$ converges to zero, we need to first derive the characteristic model of the error system given in (7) upon which the control design depends. In the following, in the absence of special instructions, we set $y_e(-1) = e_1(-1) = e_1(0) - Te_2(0)$, $e_1(i) = 0\,(\forall i < -1)$, and $e_2(i) = u(i) = 0\,(\forall i < 0)$. Then, the characteristic model of (7) can be expressed as follows.

Proposition 1. Consider the error system given in (7). If Assumptions 1–3 hold, the corresponding characteristic model can be described by the second-order time-varying difference equation,

$$y_e(k+1) = f_1(k)y_e(k) + f_2(k)y_e(k-1) + (T^2/2)b(k)u(k) + (T^2/2)b(k-1)u(k-1), \quad \forall k \geqslant 0, \tag{10}$$

where

$$f_1(k) = 2 + T^2 \left.\frac{\partial F}{\partial e_1}\right|_{(\sigma_1 e_1(k),0,k)} + T \left.\frac{\partial F}{\partial e_2}\right|_{(e_1(k),\sigma_2 e_2(k),k)}, \quad f_2(k) = -1 - T \left.\frac{\partial F}{\partial e_2}\right|_{(e_1(k),\sigma_2 e_2(k),k)}, \tag{11}$$

in which $\sigma_i \in (0,1)$ $(i = 1, 2)$ is parameters depending on the state variables $(e_1(k), e_2(k))$. Furthermore, the above time-varying parameters $\{f_1(k), f_2(k), b(k)\}$ have the following properties:

(P1) Uniform boundedness: for any $k \geqslant 0$, $[f_1(k), f_2(k), b(k)]^{\mathrm{T}} \in D$, where D is a closed convex set defined by

$$D \triangleq \left\{ (a_1, a_2, a_3)^{\mathrm{T}} \in \mathbb{R}^3 \left| \begin{array}{l} a_1 \in \left[2 - TL - T^2 L, \ 2 + TL + T^2 L\right] \\ a_2 \in \left[-1 - TL, \ -1 + TL\right] \\ a_3 \in \left[\underline{b}, \ \bar{b}_1\right] \end{array} \right. \right\}, \tag{12}$$

in which $L, \underline{b}$, and $\bar{b}_1$ are given by (2) and (3) in Assumptions 1 and 2.

(P2) Slowly time-varying property:

$$\begin{cases} |f_1(k+1) - f_1(k)| \leqslant 2(TL + T^2 L), \\ |f_2(k+1) - f_2(k)| \leqslant 2TL, \\ |b(k+1) - b(k)| \leqslant \bar{b}_2 T, \end{cases} \quad \forall k \geqslant 0, \tag{13}$$

where $\bar{b}_2$ is given by (3) in Assumption 2.

Proof. See Appendix A.

Remark 1. Various methods for deriving the characteristic model exist. Further, the description of the characteristic model is not unique. Here, we develop a constructive method to obtain the above characteristic model, so that the modeling error of the characteristic model and the stability of the controlled plant can be more conveniently analyzed below.

Remark 2. In general, the parameters of the characteristic model are uncertain, because of the uncertainties in the controlled plant. Here, the characteristic model is introduced to aid the sampled-data controller design; the simple structure of this model simplifies the controller design and the resultant control algorithm can then be more conveniently implemented in practice.

Remark 3. In the subsequent theoretical analysis, it will be verified that the error between the characteristic model and the exact discrete-time model of the system (7) can be arbitrarily small, provided that T is sufficiently small, the controller $\{u(k)\}$ guarantees that the tracking error $\{y_e(k)\}$ is uniformly bounded, and $\{T^2u(k)\}$ is uniformly bounded for any bounded $T \in (0, T_{\max}]$ $(0 < T_{\max} < \infty)$. This, to some extent, demonstrates that it is reasonable to take the difference Eq. (10) as the characteristic model, and demonstrates the validity of our control design method based on this characteristic model.

Remark 4. The parameters $\sigma_i \in (0,1)$ $(i = 1,2)$ in the time-varying coefficients $f_1(k)$ and $f_2(k)$ depend on the state variables $(e_1(k), e_2(k))$. In the absence of special instructions, the σ_1 and σ_2 terms in the following simply represent the constants located in the $(0,1)$ interval, and their values are not required to be equal.

We next present the golden-section adaptive control law based on the characteristic model given in (10). For any $k \geqslant 0$, we set the unknown parameter vector $\theta(k) \triangleq [f_1(k), f_2(k), b(k)]^{\mathrm{T}}$, the corresponding estimation vector $\hat{\theta}(k) \triangleq [\hat{f}_1(k), \hat{f}_2(k), \hat{b}(k)]^{\mathrm{T}}$, and the regression vector $\varphi(k) \triangleq [y_e(k), y_e(k-1), (T^2/2)u(k)]^{\mathrm{T}}$. Then, the golden-section adaptive control law is

$$\begin{aligned} u(k) &= \frac{2}{T^2\hat{b}(k)}\left[-l_1\hat{f}_1(k)y_e(k) - l_2\hat{f}_2(k)y_e(k-1)\right] \\ &= \frac{2}{T^2\hat{b}(k)}\left[-l_1\hat{f}_1(k)(y(k)-y^*(k)) - l_2\hat{f}_2(k)(y(k-1)-y^*(k-1))\right], \end{aligned} \tag{14}$$

where $l_1 = \frac{3-\sqrt{5}}{2} \approx 0.382$ and $l_2 = \frac{\sqrt{5}-1}{2} \approx 0.618$ are the golden-section proportions. $\hat{\theta}(k)$ is calculated from the projected gradient estimator [18], which can be expressed as

$$\hat{\theta}(k) = \pi_D\left\{\hat{\theta}(k-1) + \frac{\varphi(k-1)}{\mu + \varphi(k-1)^{\mathrm{T}}\varphi(k-1)}\left(y_e(k) - \varphi(k-1)^{\mathrm{T}}\hat{\theta}(k-1) - \frac{T^2}{2}\hat{b}(k-2)u(k-2)\right)\right\}, \tag{15}$$

where $\mu > 0$ is a parameter to be designed, $\pi_D\{x\}$ is a projection function that projects x into the set D, and D is the compact set defined by (12).

At this point, we have shown the characteristic model (10) of the error system (7) and the corresponding golden-section adaptive control (14). Moreover, it can be seen from (14) that our proposed control law has a simple linear structure, rendering it convenient for engineering applications.

3.2 Primary theorems

The performance of the closed-loop system under the golden-section adaptive controller given in (14) is demonstrated by the following theorems. For convenience, we introduce the time invariant matrix

$$A_c \triangleq \begin{bmatrix} 2(1-l_1) & -(1-l_2+2l_1) & l_2 \\ 1 & 0 & 0 \\ 0 & 1 & 0 \end{bmatrix}, \tag{16}$$

which is related to the discrete-time closed-loop equation. Our first theorem shows the exponential stability of the characteristic model (10) under (14).

Theorem 1. Consider the discrete-time closed-loop system consisting of the characteristic model (10) and the golden-section adaptive control law (14). Assuming that Assumptions 1–3 hold, there exist a positive number C_b and a sampling period $T_* > 0$ that depend on the control parameters l_1 and l_2 and the matrix A_c, such that for

$$\bar{b}_1/\underline{b} - 1 < C_b, \tag{17}$$

and $T \in (0, T_*)$, the corresponding closed-loop system is globally exponentially stable.

The stability of the controlled plant (1) and the tracking error properties are discussed below.

Theorem 2. Consider the uncertain nonlinear plant (1), the characteristic model (10), and the golden-section adaptive controller (14). Suppose that Assumptions 1–3 are satisfied, and that the parameters $\{\bar{b}_1, \underline{b}\}$ satisfy the condition given in (17). Then, for any $\rho_0 > 0$ and any initial state $\|(x_1(0), x_2(0))\| \leqslant \rho_0$, there exists $T^* > 0$ such that, for any $T \in (0, T^*)$:

(1) All trajectories satisfy

$$\sup_{t\geqslant 0}\{|x_1(t)| + T|x_2(t)|\} = O(1); \tag{18}$$

(2) The tracking performance satisfies

$$\limsup_{t\to\infty} |y(t) - y^*(t)| = O(T). \tag{19}$$

Furthermore, if $x(0) = x^*(0)$, then $|y(t) - y^*(t)| = O(T)$ holds for all $t \geqslant 0$.

Remark 5. The transient performance of the closed-loop system is related to its initial value, and a smaller initial value yields a smaller transient error. Nevertheless, for any bounded initial value, the tracking error ultimately enters the neighborhood of the origin, with a radius of $O(T)$.

Remark 6. Theoretically, the steady error can be rendered arbitrarily small by taking a sufficiently small T. However, in practice, certain limitations on the value of T exist, as a result of the various physical constraints. The corresponding stability problem with prescribed T remains a topic for further investigation.

4 Proofs of primary theorems

To prove our primary theorems, we first analyze the stability of the discrete-time closed-loop system consisting of the characteristic model (10) and the golden-section adaptive control law (14). Then, by quantitatively analyzing the error between (10) and the exact discrete-time model of the error dynamics (7), we demonstrate the performance for (7) under (14). Finally, we prove the boundedness of the hybrid closed-loop system trajectory and calculate the tracking error.

Before proceeding further, we first give the discrete-time closed-loop system consisting of (10) and (14). Substituting (14) into (10), we have

$$\begin{aligned} y_e(k+1) = &\left[f_1(k) - l_1\hat{f}_1(k)\right] y_e(k) + \left[f_2(k) - l_2\hat{f}_2(k) - l_1\hat{f}_1(k-1)\right] y_e(k-1) \\ &- l_2\hat{f}_2(k-1)y_e(k-2) + (T^2/2)\tilde{b}(k)u(k) + (T^2/2)\tilde{b}(k-1)u(k-1), \quad \forall k \geqslant 0, \end{aligned} \tag{20}$$

where $\tilde{b}(i) \triangleq b(i) - \hat{b}(i)\,(\forall i \geqslant 0)$. For the convenience of stability analysis, we derive an equivalent form for the closed-loop equation (20). We introduce the notation

$$Y_e(k+1) \triangleq \begin{bmatrix} y_e(k+1) \\ y_e(k) \\ y_e(k-1) \end{bmatrix}, \quad B_0 \triangleq \begin{bmatrix} 1 \\ 0 \\ 0 \end{bmatrix}, \quad A_k \triangleq \begin{bmatrix} \alpha_1(k) & \alpha_2(k) & \alpha_3(k) \\ 1 & 0 & 0 \\ 0 & 1 & 0 \end{bmatrix}, \tag{21}$$

where the time-varying parameters $\{\alpha_i(k),\ i = 1, 2, 3\}$ are given as

$$\alpha_1(k) = f_1(k) - l_1\hat{f}_1(k),\ \alpha_2(k) = f_2(k) - l_2\hat{f}_2(k) - l_1\hat{f}_1(k-1),\ \alpha_3(k) = -l_2\hat{f}_2(k-1),$$

and $f_i(k), \hat{f}_i(k)\,(i = 1, 2)$ are given by (11) and (15), respectively. Then, we can rewrite the closed-loop equation (20) as

$$Y_e(k+1) = A_kY_e(k) + (T^2/2)B_0\left[\tilde{b}(k)u(k) + \tilde{b}(k-1)u(k-1)\right] = A_kY_e(k) + B_0\eta_k^{\mathrm{T}}Y_e(k), \tag{22}$$

where A_k and B_0 are given by (21) and

$$\eta_k^{\mathrm{T}} \triangleq \left[-l_1\hat{f}_1(k)\tilde{b}(k)/\hat{b}(k),\ -l_2\hat{f}_2(k)\tilde{b}(k)/\hat{b}(k) - l_1\hat{f}_1(k-1)\tilde{b}(k-1)/\hat{b}(k-1),\ -l_2\hat{f}_2(k-1)\tilde{b}(k-1)/\hat{b}(k-1)\right]. \tag{23}$$

4.1 Key lemmas

We now introduce some key lemmas upon which the proof of our main results depends. Firstly, we consider the linear time-varying difference equation:

$$S(k+1) = A_k S(k), \quad \forall k \geqslant 0, \tag{24}$$

where $S(k) \triangleq [s(k), s(k-1), s(k-2)]^{\mathrm{T}} \in \mathbb{R}^3$ is the state variable and the matrix sequence $\{A_k\}$ is defined by (21). The stability of the above equation is shown below.

Lemma 1. Consider the linear time-varying difference equation given in (24). Suppose that the parameters $f_i(k)$ and $\hat{f}_i(k)$ $(i = 1, 2)$ satisfy the properties given in (12), (13), and (15). Then, there exists $T_0 > 0$ such that $\forall T \in (0, T_0]$, system (24) is exponentially stable.

Proof. See Appendix B.

As stated previously, in order to prove Theorem 2, we must quantitatively analyze the modeling error between the characteristic model (10) and the exact discrete-time model of the error plant (7). Thus, we first analyze the properties of the solution of (7). In fact, for any given sampled-data control signals $\{u(k), k \geqslant 0\}$, the solution of (7) can be expressed as

$$\begin{cases} e_1(t) = e_1(k) + (t-kT)e_2(k) + \int_{kT}^{t} (t-\tau)\left[F(e_1(\tau), e_2(\tau), \tau) + b(\tau)u(k)\right] \mathrm{d}\tau, \\ e_2(t) = e_2(k) + \int_{kT}^{t} \left[F(e_1(\tau), e_2(\tau), \tau) + b(\tau)u(k)\right] \mathrm{d}\tau, \quad \forall t \in [kT, (k+1)T]. \end{cases} \tag{25}$$

The properties of the above solution are given in the following lemma, but the proof is omitted because of space limitations.

Lemma 2. Consider the error dynamics given in (7). If Assumptions 1–3 are satisfied, for any given sampled-data control signals $\{u(k), k \geqslant 0\}$, solution (25) has the following properties:

$$\begin{aligned} z(t) \leqslant{}& p_1(t-kT)z(k) + (t-kT)p_1(t-kT)|e_2(k)| + p_2(t-kT)M_{F0} \\ &+ p_2(t-kT)b(k)|u(k)| + p_3(t-kT)\bar{b}_2|u(k)|, \end{aligned} \tag{26}$$

$$\begin{aligned} z_k(t) \leqslant{}& Lp_2(t-kT)z(k) + (t-kT)p_1(t-kT)|e_2(k)| + p_2(t-kT)\left(M_{F0} + M_{F1}\right) \\ &+ p_2(t-kT)b(k)|u(k)| + p_3(t-kT)\bar{b}_2|u(k)|, \quad \forall t \in [kT, (k+1)T], \forall k \geqslant 0, \end{aligned} \tag{27}$$

where $z(t) \triangleq |e_1(t)| + |e_2(t)|$, $z(k) \triangleq |e_1(k)| + |e_2(k)|$, and $z_k(t) \triangleq |e_1(t) - e_1(k)| + |e_2(t) - e_2(k)|$. The L, $\bar{b}_2$, M_{F0}, and M_{F1} parameters are given by (2), (3), (8), and (9), respectively, and

$$p_1(s) \triangleq \exp\left[s(2+s)L/2\right], \quad p_2(s) \triangleq \left(s + s^2/2\right)p_1(s), \quad p_3(s) \triangleq \left(s^2/2 + s^3/6\right)p_1(s). \tag{28}$$

In addition, from (25), we know that the exact discrete-time model of the error dynamics given in (7) is

$$\begin{cases} e_1(k+1) = e_1(k) + Te_2(k) + \int_{kT}^{(k+1)T} \left[(k+1)T - t\right] \cdot \left[F(e_1(t), e_2(t), t) + b(t)u(k)\right] \mathrm{d}t, \\ e_2(k+1) = e_2(k) + \int_{kT}^{(k+1)T} \left[F(e_1(t), e_2(t), t) + b(t)u(k)\right] \mathrm{d}t. \end{cases} \tag{29}$$

The following lemma shows the properties of model (29). Again, the proof is omitted because of space limitations.

Lemma 3. Consider the exact discrete-time model (29) of the error equation (7). Let Assumptions 1–3 hold. Then, Ref. (29) has the following properties:

$$\begin{cases} e_1(k+1) = f_1(k)e_1(k) + f_2(k)e_1(k-1) + (T^2/2)b(k)u(k) + (T^2/2)b(k-1)u(k-1) + \Delta_1(k+1), & \text{(30a)} \\ T|e_2(k+1)| \leqslant (1/2 + T/3)\,T^2 Lp_1(T)|e_2(k)| + \Delta_2(k+1), \quad \forall k \geqslant 0, & \text{(30b)} \end{cases}$$

where $f_1(k)$ and $f_2(k)$ have the same form as the expressions given by (11), and $\Delta_1(k+1)$ and $\Delta_2(k+1)$ satisfy

$$\begin{cases} |\Delta_1(k+1)| \leqslant c_{11}|e_1(k)| + c_{12}|e_1(k-1)| + c_{21}|e_2(k)| + c_{22}|e_2(k-1)| + c_{01}|u(k)| + c_{02}|u(k-1)| + C_1, & (31) \\ \Delta_2(k+1) = |e_1(k+1) - e_1(k)| + (1/2)T^2 Lp_1(T)|e_1(k)| + c_{03}|u(k)| + C_2, & (32) \end{cases}$$

in which the coefficients c_{ij} $(i=0,1,2, j=1,2,3)$ are positive numbers related to $\{T,\ L,\ \bar{b}_1,\ \bar{b}_2\}$ and the constants C_1 and C_2 depend on the parameters $\{T,\ L,\ M_{F0},\ M_{F1}\}$. Furthermore,

$$\begin{cases} c_{11}=\frac{1}{2}T^2L\left[1+TL\left(1+\frac{1}{3}T\right)\right]p_1(T), & c_{12}=\frac{1}{2}T^2L(1+TL)p_1(T), \\ c_{21}=\frac{1}{2}T^2L\left[1+\frac{5}{3}T+T^2L+\frac{1}{3}T^2L^2\right]p_1(T), & c_{22}=T^2L(1+TL)\left(\frac{1}{2}+\frac{T}{3}\right)p_1(T), \\ c_{01}=T^3Lp_1(T)\bar{b}_1+\frac{1}{3}T^3\bar{b}_2+O(T^4), & c_{02}=T^3L\left(\frac{1}{2}+\frac{1}{3}p_1(T)\right)\bar{b}_1+\frac{1}{3}T^3\bar{b}_2+O(T^4), \\ c_{03}=\frac{T^2}{2}\bar{b}_1+O(T^3), \quad C_2=\frac{T^2}{2}M_{F0}+O(T^3), & C_1=2T^2M_{F0}+T^2M_{F1}+O(T^3), \end{cases} \tag{33}$$

where the function $p_1(\cdot)$ is defined in (28).

4.2 Closed-loop performance analysis

We next analyze the performance of plant (1) under the golden-section adaptive controller (14) and prove our main theorems. Firstly, we show the globally exponential stability of the characteristic model given in (10) under (14).

Proof of Theorem 1. To analyze the stability of the closed-loop system (22), we first demonstrate the properties of the matrix sequence $\{A_k, k\geqslant 0\}$ by considering the time-varying difference equation (24). According to Lemma 1, we know that there exists $T_0>0$ such that $\forall T\in(0,T_0]$, equation (24) is globally exponentially stable. More specifically, by introducing the matrix sequence $\Phi(k+1,i)=A_k\Phi(k,i)$, $\Phi(i,i)=I_3$, $\forall k\geqslant i\geqslant 0$, where A_k is given by (21), and from (B8) given in the proof of Lemma 1,

$$\|\Phi(k+1,i)\|\leqslant M_0\lambda_0^{\frac{1}{2}(k+1-i)},\quad \forall k\geqslant i\geqslant 0, \tag{34}$$

where $M_0>0$ and $\lambda_0\in(0,1)$ are given by (B3). Moreover,

$$\sup_{k\geqslant 0}\|B_0\eta_k^{\mathrm{T}}\|=\sup_{k\geqslant 0}\|\eta_k\|\leqslant\delta_0(l_1,l_2)\left(\bar{b}_1/\underline{b}-1\right)+O(T), \tag{35}$$

where $\delta_0(l_1,l_2)=\sqrt{8l_1^2+2l_2^2+4l_1l_2}$. From (22), we find

$$Y_e(k+1)=\Phi(k+1,0)Y_e(0)+\sum_{i=0}^{k}\Phi(k+1,i+1)B_0\eta_i^{\mathrm{T}}Y_e(i). \tag{36}$$

Then, using (34) and (35) and applying the same calculations given in (B5)–(B8) to (36), we have

$$\|Y_e(k+1)\|\leqslant M_0\left(\sqrt{\lambda_0}+M_0\delta_0(\bar{b}_1/\underline{b}-1)+O(T)\right)^{k+1}\|Y_e(0)\|. \tag{37}$$

Therefore, setting $C_b\triangleq\left(1-\sqrt{\lambda_0}\right)/(M_0\delta_0)$ and from condition (17), we find $\sqrt{\lambda_0}+M_0\delta_0(\bar{b}_1/\underline{b}-1)<1$. Therefore, there exists $T_*\leqslant T_0$ such that $\forall T\in(0,T_*)$, $\sqrt{\lambda_0}+M_0\delta_0(\bar{b}_1/\underline{b}-1)+O(T)<1$. This result, together with (37), guarantees that the discrete-time closed-loop system given in (22), or equivalently, system (20), is globally exponentially stable. The proof is complete.

Proof of Theorem 2. We split the proof into two parts. First, we demonstrate that the sampling signals $\{x_1(k),x_2(k)\}$ of plant (1) under the golden-section adaptive controller (14) are bounded and give the explicit bounds. Then, we show the boundedness of the hybrid closed-loop system trajectories and give the tracking error.

Part I. To prove the boundedness of the state signals $\{x_1(k),x_2(k)\}$, we are simply required to prove that $\{e_1(k),e_2(k)\}$ are bounded, as the trajectories of the target system given in (4) are bounded.

Without loss of generality, we assume the initial values satisfy $|e_1(0)|+|e_2(0)|\leqslant\rho_e$, where ρ_e is determined by the upper bound of the plant's initial values ρ_0 and the target system's initial state $(x_1^*(0),x_2^*(0))$. Then, in the following, we prove that there exists a sampling period $T^*\in(0,1]$, such that $\forall T\in(0,T^*)$, the error states satisfy the properties:

$$\sup_{k\geqslant 0}|e_1(k)|\leqslant 2M_0\rho_e\triangleq\rho_1,\quad \sup_{k\geqslant 0}T|e_2(k)|\leqslant\frac{1}{1-\lambda_1}(3+(2l_1+l_2)\bar{b}_1/\underline{b})\rho_1\triangleq\rho_2, \tag{38}$$

where $M_0 > 1$, $\bar{b}_1$ and $\underline{b}$ are defined by (B3) and (3), respectively, and $\lambda_1 \in (0,1)$ is any given constant.

We adopt the contradiction argument. If we suppose the above statement is incorrect, then we know a time $k_0 \geqslant 0$ must exist such that the values of $\{e_1(k_0+1), e_2(k_0+1)\}$ do not satisfy (38). This is because the initial values satisfy $|e_1(0)| \leqslant \rho_1$ and $T|e_2(0)| \leqslant \rho_2$. Let $k^*+1 \geqslant 1$ correspond to the first time the signals $\{e_1(k),\, e_2(k)\}$ exceed the bounds given in (38). Therefore, for any $0 \leqslant k \leqslant k^*$, we have

$$|e_1(k)| \leqslant \rho_1, \quad T|e_2(k)| \leqslant \rho_2, \tag{39}$$

and at time k^*+1, only the following two cases occur:

$$|e_1(k^*+1)| > \rho_1 \quad \text{or} \quad T|e_2(k^*+1)| > \rho_2.$$

We next analyze these two cases individually.

Case 1. $|e_1(k^*+1)| > \rho_1$.

Set $E_1(k) \triangleq [e_1(k), e_1(k-1), e_1(k-2)]^{\mathrm{T}}$. According to Lemma 3 and by substituting the golden-section controller (14) into the exact discrete-time model (29), we have

$$E_1(k+1) = [A_k + B_0\eta_k^{\mathrm{T}}]E_1(k) + B_0\Delta_1(k+1), \tag{40}$$

where A_k, B_0, η_k, and $\Delta_1(k+1)$ are defined by (21), (23), and (30a), respectively, and $\Delta_1(k+1)$ satisfies (31). Next, we calculate an upper bound for $\|E_1(k^*+1)\|$. Firstly, we introduce the state transition matrix sequence $\Phi'(k+1,i) = [A_k + B_0\eta_k^{\mathrm{T}}]\Phi'(k,i)$, $\Phi'(i,i) = I_3$, $\forall k \geqslant i \geqslant 0$. From Theorem 1 and by (37), we know that under condition (17) there exists $T_* > 0$ such that $\forall T \in (0, T_*)$,

$$\|\Phi'(k+1,i)\| \leqslant M_0\lambda^{k+1-i}, \quad \forall k \geqslant i \geqslant 0, \tag{41}$$

where $M_0 > 0$ is defined by (B3) and $\lambda \in (0,1)$. Furthermore, to analyze the properties of the $\Delta_1(k+1)$ term, we split the bounds of $\Delta_1(k+1)$ into two parts, such that

$$|\Delta_1(k+1)| \leqslant \Delta_{11}(k+1) + \Delta_{12}(k+1), \tag{42}$$

where

$$\begin{cases} \Delta_{11}(k+1) = c_{11}|e_1(k)| + c_{12}|e_1(k-1)| + c_{01}|u(k)| + c_{02}|u(k-1)|, & (43)\\ \Delta_{12}(k+1) = c_{21}|e_2(k)| + c_{22}|e_2(k-1)| + C_1, & (44)\end{cases}$$

and the parameters c_{ij} $(i = 0,1,2, j = 1,2)$ and C_1 are given in (33). By substituting the golden-section control law (14) into (43), and noting that $\max\{c_{01},\, c_{02}\} = O(T^3)$, it can be easily verified that

$$\Delta_{11}(k+1) \leqslant \bar{c}_{11}|e_1(k)| + \bar{c}_{12}|e_1(k-1)| + \bar{c}_{13}|e_1(k-2)|,$$

where the parameters $\max_{1\leqslant i\leqslant 3} \bar{c}_{1i} = O(T)$. This, together with (39), indicates that

$$\Delta_{11}(k+1) = O(T), \quad \forall 0 \leqslant k \leqslant k^*. \tag{45}$$

In addition, from (33) we know that $\max\{c_{21}, c_{22}, C_1\} = O(T^2)$. This, together with (39) and (44) further indicates that $\forall 0 \leqslant k \leqslant k^*$,

$$\Delta_{12}(k+1) = O(T^2)(|e_2(k)| + |e_2(k-1)| + 1) = O(T). \tag{46}$$

Moreover, it follows from (40) that

$$E_1(k+1) = \Phi'(k+1,0)E_1(0) + \sum_{i=0}^{k} \Phi'(k+1,i+1)B_0\Delta_1(i+1). \tag{47}$$

Therefore, by substituting (41), (42), (45) and (46) into (47), we find that for any $0 \leqslant k \leqslant k^*$,

$$\|E_1(k+1)\| \leqslant \|\Phi'(k+1,0)\| \cdot \|E_1(0)\| + \sum_{i=0}^{k} \|\Phi'(k+1,i+1)\| \cdot \|B_0\| \cdot |\Delta_1(i+1)|$$

$$\leqslant M_0\lambda^{k+1}\|E_1(0)\| + \sum_{i=0}^{k} M_0\lambda^{k-i}(\Delta_{11}(i+1)+\Delta_{12}(i+1))$$
$$\leqslant M_0\|E_1(0)\| + (M_0/(1-\lambda))O(T). \tag{48}$$

Hence, by the initial condition $|e_1(0)|+|e_2(0)| \leqslant \rho_e$ and our appointment $e_1(-1)=e_1(0)-Te_2(0)$, we know there exists $T_1 \leqslant T_*$ such that for any $T\in(0,T_1)$, the inequality $\|E_1(k^*+1)\| < 2M_0\rho_e = \rho_1$ holds. Thus, we obtain a contradiction with $|e_1(k^*+1)|>\rho_1$.

Case 2. $T|x_2(k^*+1)|>\rho_2$.

Consider the inequality (30b). Firstly, for any given constant $\lambda_1\in(0,1)$, there exists $T_2\leqslant T_1$ such that for any $T\in(0,T_2]$,

$$(1/2+T/3)TLp_1(T)\leqslant\lambda_1. \tag{49}$$

We then analyze the properties of the $\Delta_2(k+1)$ term. From the analysis given in Case 1, we determined that

$$|e_1(k^*+1)|<\rho_1, \tag{50}$$

when $T\in(0,T_1)$. Thus, by substituting the control law given in (14) into (32), and from (33), (39), and (50), we find that $|\Delta_2(k+1)|\leqslant(2+(2l_1+l_2)\bar{b}_1/\underline{b})\rho_1+O(T)$ holds for any $T\in(0,T_2]$ and any $0\leqslant k\leqslant k^*$. Here, $\bar{b}_1$, $\underline{b}$, and ρ_1 are defined by (3) and (38). Therefore, from the above analysis and (30b), we know that there exists $T^*\leqslant T_2$ such that $\forall T\in(0,T^*)$ and $\forall 0\leqslant k\leqslant k^*$,

$$\begin{aligned}T|e_2(k+1)| &\leqslant \lambda_1T|e_2(k)|+(2+(2l_1+l_2)\bar{b}_1/\underline{b})\rho_1+O(T)\\ &\leqslant \lambda_1^{k+1}T|e_2(0)|+[(2+(2l_1+l_2)\bar{b}_1/\underline{b})\rho_1+O(T)]/(1-\lambda_1)\\ &\leqslant \rho_1(2+(2l_1+l_2)\bar{b}_1/\underline{b})/(1-\lambda_1)+O(T)\\ &< \rho_1(3+(2l_1+l_2)\bar{b}_1/\underline{b})/(1-\lambda_1)=\rho_2.\end{aligned} \tag{51}$$

Hence, we find that $T|e_2(k^*+1)|<\rho_2$, which contradicts the claim that $T|e_2(k^*+1)|>\rho_2$.

Thus, by combining Case 1 and Case 2, we know that $\forall T\in(0,T^*)$, the states of the exact discrete-time model (29) satisfy

$$|e_1(k)|\leqslant\rho_1,\quad T|e_2(k)|\leqslant\rho_2,\quad \forall k\geqslant 0. \tag{52}$$

In addition, from the above, we can further obtain the steady properties of the $\{e_1(k),e_2(k)\}$ states. In fact, from (48), (45) and (46),

$$\lim_{k\to\infty}\|E_1(k+1)\|\leqslant\lim_{k\to\infty}\sum_{i=0}^{k}M_0\lambda^{k-i}(|\Delta_{11}(i+1)|+|\Delta_{12}(i+1)|)=\frac{M_0}{1-\lambda}O(T)=O(T). \tag{53}$$

Hence, there exists $N_0(T)\in\mathbb{N}$ such that

$$|e_1(k)|=O(T),\quad \forall k\geqslant N_0(T). \tag{54}$$

Moreover, for the $e_2(k)$ state and from (32), (33), and (54), we know that for any $k\geqslant N_0(T)$, $|\Delta_2(k+1)|=O(T)$. Together with (30b) and (49), this indicates that $\forall T\in(0,T^*)$ and $\forall k\geqslant N_0(T)$,

$$\begin{aligned}T|e_2(k+1)|\leqslant\lambda_1T|e_2(k)|+|\Delta_2(k+1)| &\leqslant \lambda_1^{k+1-N_0}T|e_2(N_0)|+\sum_{i=N_0}^{k}\lambda_1^{k-i}|\Delta_2(i+1)|,\\ &\leqslant \lambda_1^{k+1-N_0}T|e_2(N_0)|+O(T).\end{aligned}$$

Thus, it can be determined that

$$\lim_{k\to\infty}T|e_2(k)|=O(T), \tag{55}$$

that is, $\lim_{k\to\infty}|e_2(k)|=O(1)$.

To summarize, we have shown the boundedness of the $\{e_1(k),e_2(k)\}$ state signals and given the explicit bounds (52). Also, we have provided the corresponding steady properties (53) and (55).

Part II. In this part, we analyze the properties of the trajectory of the closed-loop system consisting of the error dynamics (7) and the control law (14), and we give the tracking error.

For the solution (25) of the error system given in (7), according to Assumptions 1–3 and using (8), we find that for any $k \geqslant 0$ and any $t \in [kT, (k+1)T]$,

$$|e_1(t)| \leqslant |e_1(k)| + T|e_2(k)| + L\int_{kT}^{t}(t-\tau)z(\tau)\mathrm{d}\tau + (T^2/2)b(k)|u(k)| + (T^3/6)\bar{b}_2|u(k)| + (T^2/2)M_{F0}, \quad (56)$$

where $z(t)$ is defined in Lemma 2 and satisfies (26), and $\bar{b}_2$ and M_{F0} are defined by (3) and (8), respectively. Then, by substituting (14) and the inequality (26) into (56), and from the bounds given in (52), we find that for any $t \geqslant 0$ and $T \in (0, T^*)$,

$$|e_1(t)| \leqslant (1 + (2l_1 + l_2)\bar{b}_1/\underline{b})\rho_1 + \rho_2 + O(T). \quad (57)$$

Similarly, according to Assumptions 1–3 and using (25), (14), (8), and (26), we have $\forall t \geqslant 0$ and $\forall T \in (0, T^*)$,

$$T|e_2(t)| \leqslant 2(2l_1 + l_2)(\bar{b}_1/\underline{b})\rho_1 + \rho_2 + O(T). \quad (58)$$

Consequently, from (57) and (58) the trajectory of the closed-loop system satisfies

$$|e_1(t)| + T|e_2(t)| = O(1), \quad \forall t \geqslant 0. \quad (59)$$

This, together with the boundedness of the target trajectory $(x_1^*(t), x_2^*(t))$, indicates that Eq. (18) is true.

Moreover, for the solution (25) of the error system given in (7), according to Lemma 2 and from the steady properties of the $\{e_1(k), e_2(k)\}$ signals given by (53) and (55), along with the boundedness of the $\{e_1(t), e_2(t)\}$ states given by (59), it can easily be seen that

$$\lim_{t\to\infty}[|e_1(t)| + T|e_2(t)|] = O(T). \quad (60)$$

Therefore, from (60), the tracking error satisfies (19). Furthermore, if the initial condition satisfies $x(0) = x^*(0)$, then $e_1(0) = e_2(0) = 0$. Hence, from the above analysis and by (48) and (51), it is apparent that the bounds ρ_1 and ρ_2 in this case satisfy the statements that $\rho_1 = O(T)$ and $\rho_2 = O(T)$. Therefore, according to (57) and (58), it can be shown that

$$|e_1(t)| + T|e_2(t)| = O(T), \quad \forall t \geqslant 0. \quad (61)$$

From the above, the proof of Theorem 2 is complete.

5 Simulation

We illustrate the performance of the proposed control method using two numerical examples. The first is based on a practical plant, whereas the second example is an academic case with strong nonlinearity.

Example 1. We consider pitch-axis attitude control for a three-axis stabilized satellite with liquid propellant and flexible solar arrays during motor operation. The system can be simply modeled as $I(t)\ddot{\theta}_p = u + d(t)$, $y = \theta_p$, where $\theta_p \in \mathbb{R}$ denotes the pitch angle, $u \in \mathbb{R}$ is the control input, $I(t)$ denotes the total moment of inertia (the value of which varies over time as result of the change in the satellite center), and $d(t)$ represents the disturbances causing by the liquid propellant and flexible solar arrays. Here, we take $I(t) = I_0 + I_1\delta_I(t)$, where $I_0 = 1000\ \mathrm{kg}\cdot\mathrm{m}^2$, $I_1 = 10\% I_0$, and $|\delta_I(t)| \leqslant 1$ with a bounded derivative. In addition, we take $d(t) = \sum_{i=1}^{100} C_i^* \sin(\omega_i^* t + p_i^*)$ to equivalently describe the disturbance where $C_i^*/I_0 \in (0, 20]$, $\omega_i^* \in (0, 50]$, and $p_i^* \in [0, 2\pi]$ $(i = 1, \ldots, 100)$ are random numbers. The goal is to have θ_p asymptotically track the reference signal generated by the target system

$$\dot{x}_1^* = x_2^*, \quad \dot{x}_2^* = -2w_0 x_2^* - w_0^2 x_1^* + r(t), \quad y^* = x_1^*, \quad (62)$$

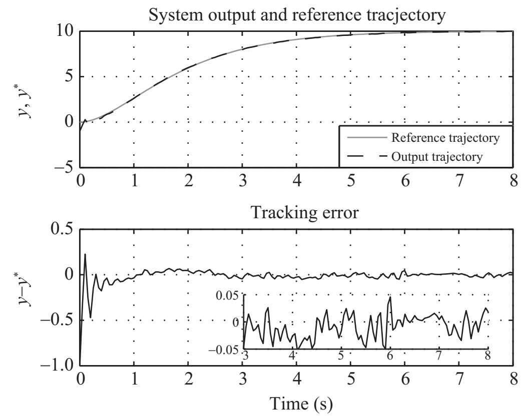

Figure 1 System output, reference trajectory, and corresponding tracking error ($\theta_p(0) = -1$).

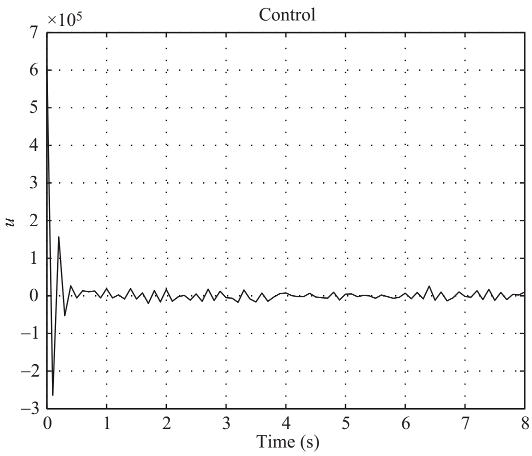

Figure 2 Control signal ($\theta_p(0) = -1$).

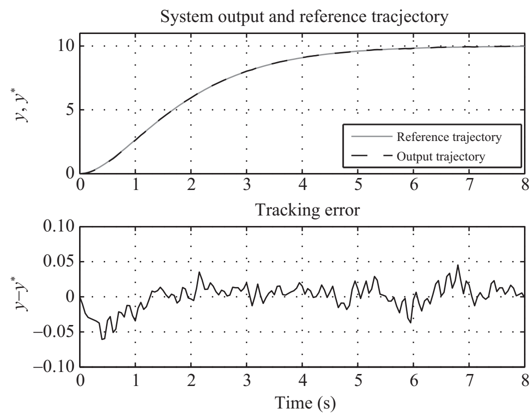

Figure 3 System output, reference trajectory, and corresponding tracking error ($\theta_p(0) = 0$).

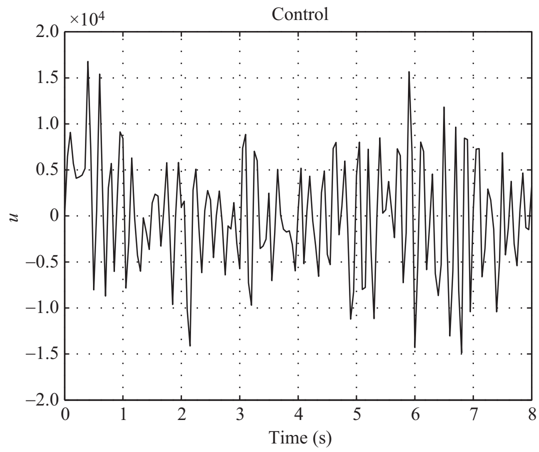

Figure 4 Control signal ($\theta_p(0) = 0$).

where the parameters $w_0 = 1$ and $r(t) = 10$ and the initial condition is $x_1^*(0) = 0$. Then, the corresponding characteristic model, as given by (10), is $y_e(k+1) = 2y_e(k) - y_e(k-1) + (T^2/2)[b(k)u(k) + b(k-1)u(k-1)]$, where $y_e(k) = y(k) - y^*(k)$ and $b(k) = 1/I(k) \in [1/1100, 1/900]$. Further, the golden-section adaptive control is $u(k) = -2[2l_1((y(k) - y^*(k)) - l_2(y(k-1) - y^*(k-1))]/(T^2\hat{b}(k))$, where $l_1 = 0.382$, $l_2 = 0.618$, and $\hat{b}(k)$ is calculated using the projected gradient algorithm. Thus, by taking $T = 0.05$, the tracking performance and the control signals for the initial values $\theta_p(0) = -1$ and $\theta_p(0) = 0$ can be obtained, as shown in Figures 1 and 2 and Figures 3 and 4, respectively.

It is apparent that, in both cases, the tracking performance of the closed-loop systems can meet the requirements. Furthermore, the transient performance is improved as the initial error decreases, which coincides with our theoretical results.

Example 2. Consider the nonlinear system

$$\dot{x}_1 = x_2, \quad \dot{x}_2 = \frac{x_1 x_2 \sin x_1}{2 + x_1^2} + \frac{3x_1 x_2^3}{(1 + x_2^4)\mathrm{e}^{x_1^2 + 5x_2^2}} + (2 + \sin 10t)u + d(t), \quad y = x_1,$$

where $d(t) = 1$. Similar to the previous example, the control objective is to have y asymptotically track the reference signal generated by the target system (62), with $w_0 = 1$, $r(t) = \sin t$, and $x_1^*(0) = 0$. Hence, the characteristic model is described by: $y_e(k+1) = f_1(k)y_e(k) + f_2(k)y_e(k-1) + (T^2/2)[b(k)u(k) + b(k-1)u(k-1)]$, where $\{f_1(k), f_2(k), b(k)\}$ satisfy $|f_1(k) - 2| \leqslant 3(T + T^2)$, $|f_2(k) + 1| \leqslant 3T$, and $1 \leqslant b(k) \leqslant 3$.

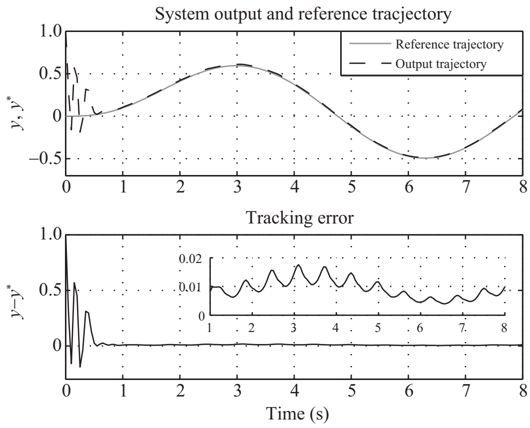

Figure 5 System output, reference trajectory, and corresponding tracking error ($T = 0.05$).

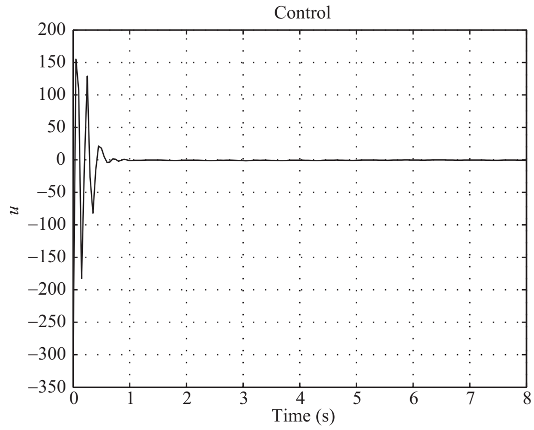

Figure 6 Control signal ($T = 0.05$).

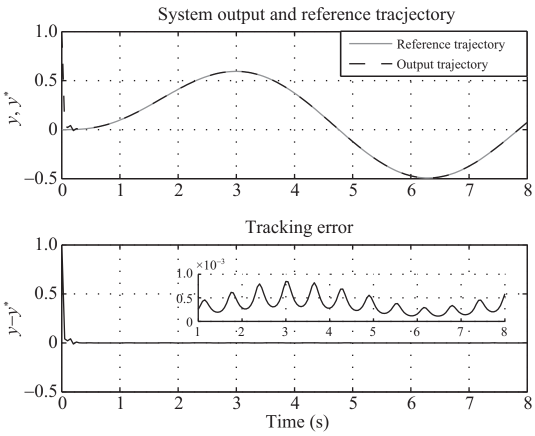

Figure 7 System output, reference trajectory, and corresponding tracking error ($T = 0.01$).

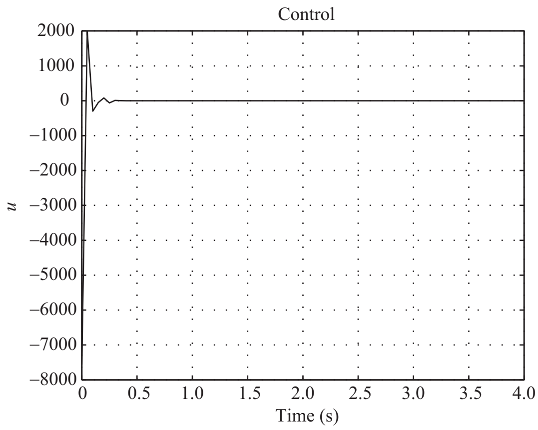

Figure 8 Control signal ($T = 0.01$).

Furthermore, we have the golden-section adaptive control $u(k) = -2[l_1\hat{f}_1(k)((y(k)-y^*(k))+l_2\hat{f}_2(k)(y(k-1)-y^*(k-1))]/(T^2\hat{b}(k))$, where the parameter estimates $\{\hat{f}_1(k), \hat{f}_2(k), \hat{b}(k)\}$ are given by the estimator of (15). By taking $x_1(0) = 1$, the tracking errors and control signals for $T = 0.05$ and $T = 0.01$ can be obtained, as shown in Figures 5 and 6 and Figures 7 and 8, respectively. As expected, such uncertain nonlinearity can be managed by the proposed $u(k)$. Further, by comparing Figure 5 with Figure 7, we find that the steady-state tracking error decreases as T is reduced. All of the above findings are consistent with the theoretical results, illustrating the efficacy of the proposed control method.

6 Conclusion

The purpose of this paper is to deal with the tracking problem for a class of second-order nonlinear systems, which are subjected to both unknown nonparametric dynamics and external disturbances, using sampled-data output feedback. The characteristic modeling method is used to design the sampled-data control law; this is achieved by first deriving the characteristic model and then proposing the corresponding golden-section adaptive control law. We also prove the following three properties: Firstly, the characteristic model under the golden-section adaptive controller is globally exponentially stable; secondly, the trajectory of the hybrid closed-loop system is bounded; and thirdly, the output tracking error can be arbitrarily small if the sampling period is chosen to be sufficiently small. In addition, the stability condition given in this work depends on the parameters of the plant, the controller parameters, and the sampling period only which, to the best of the authors' knowledge, appears to be the weakest criterion. Two numerical examples are also given to illustrate the validity of our proposed sampled-data output feedback controller. All the above results confirm the theoretical basis of the characteristic modeling method, and also lay important theoretical foundations for practical applications of this technique. Of course, a number of problems requiring further investigation remain, particularly those concerning more general cases.

Acknowledgements This work was supported by National Natural Science Foundation of China (Grant No. 61333008) and National Key Basic Research and Development Program of China (973) (Grant No. 2013CB733100).

Conflict of interest The authors declare that they have no conflict of interest.

References

1 Wu H X, Hu J, Xie Y C. Characteristic Model Based Intelligent and Adaptive Control (in Chinese). Beijing: China Science and Technology Press, 2009
2 Wu H X. All Coefficient Adaptive Control Theory and Applications (in Chinese). Beijing: National Defense Industry Press, 1990
3 Wu H X, Hu J, Xie Y C. Characteristic model-based all-coefficient adaptive control method and its applications. IEEE Trans Syst Man Cybern Part C–Appl Rev, 2007, 37: 213–221
4 Hu J. All coefficient adaptive re-entry lifting control of manned spacecraft (in Chinese). J Astron, 1998, 19: 8–12
5 Hu J, Xie Y C. The all coefficient adaptive control of spacecraft instantaneous thermal current (in Chinese). Contr Theor Appl, 1997, 14: 685–690
6 Wang Y C, Geng C F, Wu H X. An adaptive fuzzy controller and its application in the process control of aluminum electrolysis (in Chinese). Aerosp Contr, 2001, 19: 21–26
7 Hu J, Xie Y C, Zhang H, et al. Shenzhou-8 spacecraft guidance, navigation and control system and flight result evaluation for rendezvous and docking (in Chinese). Aerosp Contr Appl, 2011, 37: 1–5
8 Xie Y C, Hu J, Wang M, et al. Accurate and stable control of Shenzhou spacecraft in rendezvous and docking. In: Proceedings of the 19th IFAC Symposium on Automatic Control in Aerospace, Wuerzburg, 2013. 524–528
9 Meng B, Wu H X. Proof of the characteristic model of the linear time invariant systems (in Chinese). Sci China Ser F-Inf Sci, 2007, 37: 1258–1271
10 Meng B, Wu H X. On characteristic modeling of a class of flight vehicles' attitude dynamics. Sci China Tech Sci, 2010, 53: 2074–2080
11 Xie Y C, Wu H X. The application of the golden section in adaptive robust controller design. Chinese J Autom, 1992, 4: 197–205
12 Wu H X, Wang Y, Xie Y C. Nonlinear golden-section adaptive control (in Chinese). J Astron, 2002, 23: 1–8
13 Hu J. Golden-section control of the second-order plant with unknown input delay (in Chinese). Aerosp Contr Appl, 2014, 40: 1–7
14 Huang H, Zhang Z. Characteristic model-based H_2/H_∞ robust adaptive control during the re-entry of hypersonic cruise vehicles. Sci China Inf Sci, 2015, 58: 012202
15 Wang Y. Stability analysis of characteristic model based all-coefficient adaptive method for a class of minimum-phase nonlinear systems (in Chinese). Contr Theor Appl, 2012, 29: 1097–1107
16 Huang J F, Kang Y, Meng B, et al. Characteristic model based adaptive controller design and analysis for a class of SISO systems. Sci China Inf Sci, in press. doi: 10.1007/s11432-015-5310-1
17 Horn R A, Johnson C R. Matrix Analysis. New York: Combridge University Press, 1985
18 Guo L. Time-Varying Stochastic Systems–Stability, Estimation and Control (in Chinese). Jilin: Jilin Science and Technology Press, 1992

Appendix A Proof of Proposition 1

For any given sampling rate $T > 0$, based on the core concept of characteristic modeling (i.e., that the characteristics of the system are retained), and combining the exact discrete-time model of the error system given in (7), we extract the following discrete-time model:

$$e_1(k+1) = e_1(k) + Te_2(k+1) - (T^2/2)b(k)u(k), \quad e_2(k+1) = e_2(k) + TF(e_1(k), e_2(k), k) + Tb(k)u(k). \tag{A1}$$

Then, according to Assumption 1 and by the mean-value theorem, we have

$$F(e_1(k), e_2(k), k) = F(0,0,k) + (\partial F/\partial e_1)|_{(\sigma_1 e_1(k),0,k)} \cdot e_1(k) + (\partial F/\partial e_2)|_{(e_1(k),\sigma_2 e_2(k),k)} \cdot e_2(k), \tag{A2}$$

where σ_1, $\sigma_2 \in (0,1)$ are parameters depending on the state variables $(e_1(k), e_2(k))$. Substituting (A2) into the difference equation (A1), and noting that $y_e(-1) = y_e(0) - Te_2(0)$, $u(-1) = 0$, we obtain $\forall k \geqslant 0$,

$$y_e(k+1) = f_1(k)y_e(k) + f_2(k)y_e(k-1) + (T^2/2)b(k)u(k) + (T^2/2)b(k-1)u(k-1)$$

$$+ T^2F(0,0,k) + (T^2/2)h(k)b(k-1)u(k-1), \tag{A3}$$

where $f_1(k)$ and $f_2(k)$ are given by (11) and $h(k) \triangleq T\,(\partial F/\partial e_2)|_{(e_1(k),\sigma_2 e_2(k),k)}$. As the last two terms in (A3) have the properties that $T^2F(0,0,k) = O(T^2)$ and $h(k) = O(T)$, we obtain the characteristic model of (10) by omitting the final two terms in Eq. (A3).

Furthermore, from Assumption 1, we know that $|\partial F/\partial e_i| = |\partial f/\partial x_i| \leqslant L$ $(i = 1, 2)$ which, together with Assumption 2, further ensures that the time-varying parameters of (10) are uniformly bounded and belong to the set D defined by (12). In addition, from (12) and Assumption 2, we know that the slow time-varying property of parameters $\{f_1(k), f_2(k), b(k)\}$ given by (13) holds. Thus, the proof is complete.

Appendix B Proof of Lemma 1

First, we rewrite (24) as

$$S(k+1) = A_kS(k) = A_cS(k) + B_0\zeta_k(S(k)), \tag{B1}$$

where A_k, B_0, and A_c are defined by (21) and (16), respectively, and the function $\zeta_k(\cdot)$ is defined by

$$\zeta_k(S(k)) = \Big[\big(f_1(k) - 2\big) + l_1\big(2 - \hat{f}_1(k)\big)\Big]\,s(k) + \Big[\big(1 + f_2(k)\big) - l_2\big(1 + \hat{f}_2(k)\big) + l_1\big(2 - \hat{f}_1(k-1)\big)\Big]\,s(k-1) - l_2\big(1 + \hat{f}_2(k-1)\big)s(k-2), \tag{B2}$$

For the matrix A_c, according to the Jury criterion[1)], the eigenvalues are located in the unit circle with the parameters $l_1 = \frac{3-\sqrt{5}}{2}$ and $l_2 = \frac{\sqrt{5}-1}{2}$. Therefore, by setting $\rho(A_c) = \max\limits_{1\leqslant i\leqslant 3}\{\,|\lambda_i(A_c)|\,\}$, we find $\rho(A_c) < 1$. Furthermore, from [18], there exist

$$M_0 = \sqrt{3}\left(1 + \frac{2}{\epsilon_0}\right)^2 \text{ and } \lambda_0 = \rho(A_c) + \epsilon_0\|A_c\| < 1, \tag{B3}$$

with a certain small constant $\epsilon_0 > 0$, such that

$$\|A_c^k\| \leqslant M_0\lambda_0^k, \quad \forall k \geqslant 0. \tag{B4}$$

In addition, from the difference equation (B1), we have

$$S(k+1) = A_c^{k+1}S(0) + \sum_{i=0}^{k} A_c^{k-i}B_0\zeta_i(S(i)). \tag{B5}$$

Moreover, from (B2) along with the uniform boundedness for $f_1(k)$ and $f_2(k)$ given in (12) and that for $\hat{f}_1(k)$ and $\hat{f}_2(k)$ given in (15), there exists a positive number $c_0 > 0$ that depends on l_1 and l_2 only, such that

$$|\zeta_k(S(k))| \leqslant c_0TL\|S(k)\|. \tag{B6}$$

Thus, substituting (B6) into (B5) and from (B4), we have

$$\|S(k+1)\| \leqslant \|A_c^{k+1}S(0)\| + \sum_{i=0}^{k}\|A_c^{k-i}B_0\zeta_i(S(i))\| \leqslant M_0\lambda_0^{k+1}\|S(0)\| + \sum_{i=0}^{k} M_0\lambda_0^{k-i}c_0TL\|S(i)\|.$$

Let $d_0 \triangleq \frac{M_0}{\lambda_0}c_0TL$. Then, according to the Bellman-Gronwall inequality [18], we have

$$\lambda_0^{-(k+1)}\|S(k+1)\| \leqslant M_0\|S(0)\|\left[1 + d_0\sum_{i=0}^{k}(1+d_0)^{k-i}\right] \leqslant M_0\|S(0)\|\,(1+d_0)^{k+1} \leqslant M_0\|S(0)\|\exp\left(d_0(k+1)\right). \tag{B7}$$

Therefore, let $T \leqslant -\lambda_0\ln(\lambda_0)/(2c_0M_0L) \triangleq T_0$, which ensures $\exp\left(d_0(k+1)\right) \leqslant \lambda_0^{-(k+1)/2}$. This, together with (B7), ensures that the solution of (B1) satisfies

$$\|S(k+1)\| \leqslant M_0\lambda_0^{\frac{k+1}{2}}\|S(0)\| = M_0\exp\left\{-\lambda_*(k+1)\right\}\|S(0)\|, \tag{B8}$$

where $\lambda_* \triangleq \frac{1}{2}\ln\left(\frac{1}{\lambda_0}\right)$. Therefore, for any $T \in (0, T_0]$, the difference equation (B1) is globally exponentially stable. Thus, the lemma is true.

1) Hu S S. Automatic Control (in Chinese). 5th ed. Beijing: Science Press, 2007.